


RESEARCH

Open Access



Cell membrane fluidity and ROS resistance define DMSO tolerance of cryopreserved synovial MSCs and HUVECs

Mitsuru Mizuno^{1*} , Takahisa Matsuzaki^{2,3,4}, Nobutake Ozeki¹, Hisako Katano¹, Hideyuki Koga⁵, Takanori Takebe^{3,6,7,8,9}, Hiroshi Y. Yoshikawa^{2,4,10} and Ichiro Sekiya¹

Abstract

Objectives: Synovial mesenchymal stem cells (MSCs) have high freeze–thaw tolerance, whereas human umbilical vein endothelial cells (HUVECs) have low freezing tolerance. The differences in cell type-specific freeze–thaw tolerance and the mechanisms involved are unclear. This study thus aimed to identify the biological and physical factors involved in the differences in freeze–thaw tolerance between MSCs and HUVECs.

Materials and methods: For biological analysis, MSC and HUVEC viability after freeze-thawing and alteration of gene expression in response to dimethyl sulfoxide (DMSO, a cryoprotectant) were quantitatively evaluated. For physical analysis, the cell membrane fluidity of MSCs and HUVECs before and after DMSO addition was assessed using a histogram for generalized polarization frequency.

Results: HUVECs showed lower live cell rates and higher gene expression alteration related to extracellular vesicles in response to DMSO than MSCs. Fluidity measurements revealed that the HUVEC membrane was highly fluidic and sensitive to DMSO compared to that of MSCs. Addition of CAY10566, an inhibitor of stearyl-coA desaturase (*SCD1*) that produces highly fluidic desaturated fatty acids, decreased the fluidity of HUVECs and increased their tolerance to DMSO. The combination of CAY10566 and antioxidant glutathione (GSH) treatment improved HUVEC viability from 57 to 69%. Membrane fluidity alteration may thus contribute to pore-induced DMSO influx into the cytoplasm and reactive oxygen species production, leading to greater cytotoxicity in HUVECs, which have low antioxidant capacity.

Conclusions: Differences in freeze–thaw tolerance originate from differences in the cell membranes with respect to fluidity and antioxidant capacity. These findings provide a basis for analyzing cell biology and membrane-physics to establish appropriate long-term preservation methods aimed at promoting transplantation therapies.

Keywords: Cell membrane fluidity, ROS resistance, Cryopreserve, Mesenchymal stem cells, Human umbilical vein endothelial cells

Introduction

Mesenchymal stem cells (MSCs) are a promising source for cell therapy; however, the development of a long-term preservation technology for processed cells is necessary for their widespread use. Cryopreservation is the most common method for long-term cell preservation [1, 2]. Synovial MSCs have high freeze–thaw tolerance and can maintain their chondrogenic differentiation potential

*Correspondence: mizuno.arm@tmd.ac.jp

¹ Center for Stem Cell and Regenerative Medicine, Tokyo Medical and Dental University (TMDU), 1-5-45, Bunkyo-ku, Yushima, Tokyo 113-8510, Japan

Full list of author information is available at the end of the article



even after freezing and thawing [3]. These cells, immediately after freezing and thawing, have the same treatment effect as cultured cells when administered to a knee osteoarthritis model [4]. However, it is not clear why MSCs retain this high freeze–thaw tolerance. On the contrary, various cell types with low freeze–thaw tolerance are known; these include human umbilical vein endothelial cells (HUVECs) [5]. HUVECs belong to the endothelial lineage and are expected to be used a cell source for liver [6] and cartilage regeneration [7]. However, to achieve long-term practical use and for developing long-term preservation technologies for cells with low freeze–thaw tolerance, the molecular mechanism underlying cell type-specific freeze–thaw tolerance needs to be clarified.

Cryoprotectants have been used to prevent the cell damage caused by cryopreservation. Among the commonly used cryoprotectants, dimethyl sulfoxide (DMSO) is the most common [8, 9]. DMSO addition is intended to increase the osmotic pressure in the cryopreservation solution, thereby causing loss of water from cells with reduced formation of ice clumps inside cells and damage to intracellular organelles [10–12]. In contrast, the toxicity of DMSO itself to cells has also been reported in several studies [13, 14]. DMSO toxicity is correlated with alterations in gene expression profiles and generation of reactive oxygen species (ROS) [15–17]. DMSO shows a wide range of toxicity depending on cell type, and this difference in toxicity may originate from the biological and physical characteristics of the cells, resulting in differences in freeze–thaw tolerance.

The cell membrane is the first contact interface for DMSO. Under physiological conditions, the cell membrane is in a highly fluid state with abundant lipids, which broadens the diversity of cellular functions. Fluidity is one of the representative physical properties of the cell membrane, and its values varies among cell types [18]. Membrane fluidity has been considered to contribute to fundamental cellular functions such as cell adhesion [19] and migration [20, 21]. Although membrane fluidity is an important factor that influences the cryopreservation quality of sperm [22, 23], the impact of membrane fluidity on the cryopreservation quality of various cells other than germ cells is not well assessed. Furthermore, the effect of DMSO on the membrane fluidity of somatic cells, especially synovial MSCs and HUVECs, has not been clearly evaluated.

Analyzing the effects of DMSO on two types of cells with different freeze–thaw tolerances may facilitate identification of biological and physical factors involved in the different freeze–thaw tolerance characteristics. Thus, this study aimed to identify the biological and physical factors

contributing to the different freeze–thaw tolerance of MSCs and HUVECs.

Materials and methods

Synovial MSCs and HUVECs

This study was approved by the Medical Research Ethics Committee of Tokyo Medical and Dental University (M2017-142), and all subjects provided informed consent. The human synovium was harvested from the knees of six female donors (55–81 years) with osteoarthritis, during total knee arthroplasty. The synovial cells were cultured as previously reported [24]. Briefly, the synovium was digested in a solution of 3 mg/mL collagenase (Sigma-Aldrich Co. LLC, Merck KGaA, Darmstadt, Germany) at 37 °C. After 3 h, the digested cells were filtered through a 70 µm cell strainer (Greiner Bio-One GmbH, Frickenhausen, Germany). The cells were cultured in α -minimum essential medium (α -MEM; Thermo Fisher Scientific, MA, USA) supplemented with 1% antibiotic–antimycotic (Thermo Fisher Scientific) and 10% fetal bovine serum in a cell culture incubator (Astec Co., Ltd., Fukuoka, Japan) at 37 °C under 5% CO₂.

HUVECs from four donors were purchased from Life-line® Cell Technology (CA, USA) and maintained in Endothelial Cell Growth Medium 2 (PromoCell GmbH, Heidelberg, Germany).

Freeze-thawing

Synovial MSCs and HUVECs (3×10^5 cells) were suspended in 250 µL of 95% FBS and 5% DMSO (Fujifilm Wako Pure Chemical Corporation, Tokyo, Japan). Freezing and thawing were performed as follows: first, the tubes containing the cells were placed in a bio-freezing vessel (Bicell, Japan Freezer, Tokyo, Japan); second, the frozen cells were thawed using a frozen cell thawing device (ThawSTAR, BioLife Solutions, WA, USA); third, the cell suspensions were diluted to 1 mL by slow dropping of 750 µL cold medium and used for analysis without washing. The cells were stored at –150 °C for at least 1 month before analysis.

Quantification of live cells

Flow cytometry was performed using the CellEvent® Caspase-3/7 Green Flow Cytometry Assay Kit (Thermo Fisher Scientific) and SYTOX™ blue dead cell stain (Thermo Fisher Scientific) on a FACS Verse system (Becton, Dickinson and Company; BD, NJ, USA). Briefly, the cells were suspended at 3×10^5 cells/mL and stained for 30 min at 37 °C with caspase-3/7 Green in the dark. FITC-V500⁻ cells were evaluated as live cells. These data were analyzed using FlowJo software (Tree Star Inc., CA, USA).

RNA, DNA, and protein quantification

Cultured and thawed synovial MSCs and HUVECs (3×10^5 cells) were suspended in 250 μ L of 95% FBS and 5% DMSO (Fujifilm Wako Pure Chemical Corporation, Tokyo, Japan). Total RNA, DNA, and protein were extracted from the cells using an AllPrep DNA/RNA/Protein Mini Kit according to the manufacturer's instructions (Qiagen N.V., Venlo, The Netherlands). RNA and DNA concentrations were measured using a NanoDrop 1000 instrument (Thermo Scientific). Protein concentrations were determined using a Pierce BCA protein assay kit (Thermo Fisher Scientific).

Colony forming unit (CFU) assay

For colony formation assays, cells were plated at 100 cells per 9.6 cm². The wells were stained with 1% crystal violet (Fujifilm Wako Pure Chemical Industries, Osaka, Japan) after 12 and 10 days for MSCs and HUVECs, respectively. To compare the number of colonies, 18 replicates and three independent experiments were performed. One representative well is shown, and the number of colonies was counted manually. The colonies were imaged using a microscope (BZ-X700, Keyence Co., Ltd., Osaka, Japan) for further quantification. Image J software (National Institutes of Health, MD, USA) was used to quantify the crystal violet-positive area. The violet color was defined by selecting one violet area and then selecting the Image/Adjust/Color threshold tool and the Sample button. The image was then converted into an 8-bit binary image, and the crystal violet-positive area was calculated.

RNA-seq

Total RNA was extracted from synovial MSCs and HUVECs using an RNeasy Mini Kit (Qiagen N.V.). RNA sequencing was performed as described previously [25]. Briefly, the RNA concentration and quality were determined using a Quantus Fluorometer (Promega Co., WI, USA) and an Agilent 2100 Bioanalyzer, respectively. All samples had an RNA integrity number >7. Sequencing libraries were prepared using the Agilent SureSelect Strand-Specific RNA Library Prep (for Illumina). Briefly, poly-A RNA was purified from 300 ng of total RNA per sample using oligo-dT magnetic beads. The libraries were amplified by PCR for 13 cycles and were then purified using AMPure XP beads. The libraries were sequenced on an Illumina HiSeq1500 system using single-end 50 bp reads.

To analyze the altered genes, Venn diagram-based analysis and GO (gene ontology) term enrichment analyses were performed. Venn diagrams were generated for

genes that were increased by more than twofold after DMSO supplementation using Venny software. The representative GO terms from the top 15 or 20 gene clusters were revealed using the Database for Annotation, Visualization and Integrated Discovery (DAVID) [26].

Among the 30,134 genes analyzed by RNA-seq, antioxidant-related genes determined using hierarchical clustering analysis and the genes in the pathway GO1903561 (extracellular vesicles) are shown. A heatmap was generated for genes showing more than two copies.

Cell membrane fluidity measurements

We used dimethyl-6-dodecanoyl-2-naphthylamine (Laurdan, AdipoGen Life Science, CA, USA) as a probe for the quantitative evaluation of cell membrane fluidity [18, 27–29]. The lauridan powder was dissolved in DMSO (9 mM final), and the solution was diluted in RPMI 1640 medium (33 μ M final concentration). Cells in the medium were incubated for 30 min at ambient temperature. Fluorescence images of cells were captured by a confocal microscope (TCS-SP8, Leica Microsystems, Wetzlar, Germany) equipped with a $\times 10$ objective lens ($NA = 0.75$) at ambient temperature. For lauridan extraction, a 405-nm laser diode was utilized as a light source. To evaluate membrane fluidity as a generalized polarization (GP) value, the fluorescence intensities at 406–460 nm ($I_{406-460}$) and 470–530 nm ($I_{470-530}$) were obtained using a spectrum analyzer in the confocal unit. The GP values were defined as follows:

$$GP = \frac{I_{406-460} - G \times I_{470-530}}{I_{406-460} + G \times I_{470-530}} \quad (1)$$

and G values were calibration factors, defined as:

$$G = \frac{GP_{meas} + 1}{GP_{meas} - 1} \div \frac{GP_{ref} + 1}{GP_{ref} - 1} \quad (2)$$

As a reference GP value for lauridan, $GP_{ref} = 0.207$ was used [18, 29]. The measured GP of lauridan in DMSO solution (33 μ M in final) was used for GP_{meas} by using $G = 1$ in Eq. 1. The histograms for GP frequency were calculated from images of at least 30 cells per donor.

Measurement of glutathione (GSH) and superoxide dismutase (SOD)

GSH was determined using a total glutathione quantification kit (Dojindo Laboratories, Kumamoto, Japan) according to the manufacturer's instructions. Briefly, the cells were cultured and harvested. Then, 1.0×10^6 cells were lysed by adding 10 mM HCl, frozen and thawed twice, added 5% sheep serum albumin, and centrifuged.

The supernatant was used for the GSH assay following the manufacturer's protocol. The absorbance of the solution at 405 nm was measured using a plate reader (Infinite M200; Tecan, Männedorf, Switzerland).

Time course alteration of GSH was determined using cultured cells in a 96-well plate. The cells were fixed and stained at each time point using ThiolTracker™ (Thermo Fisher Scientific) and their fluorescence was measured using a plate reader. The relative fluorescence unit (RFU) values of GSH per well were standardized by counting the RFUs of propidium iodide (Miltenyi Biotech, Bergish Gladbach, Germany), and the standardized RFUs were calculated as RFUs of GSH relative to time 0. The cells were also stained with ThiolTracker and observed under a microscope (BZ-X700).

SOD activity was examined using the SOD assay kit-WST (DOJINDO LABORATORIES), according to the manufacturer's instructions. Briefly, cells were cultured, and 1.0×10^6 cells were harvested. The cells were homogenized to break the cell membrane, PBS was added, and the samples were centrifuged. The supernatant was used for the SOD assay following the manufacturer's protocol. The absorbance of the solution at 450 nm was measured using a plate reader.

Observation and quantification of ROS

At 0 and 3 h after supplementation with 5% DMSO, the cells were fixed with 4% paraformaldehyde and stained using CellROX® Green Reagent (Thermo Fisher Scientific). The cells were counterstained with 4,6-diamidino-2-phenylindole (DAPI; Fujifilm Wako) and analyzed under a microscope. Time course alteration of GSH was determined for cultured cells in a 96-well plate using a plate reader. The cells were fixed and measured at each time point using CellROX® Green Reagent. The RFU values of ROS per well were standardized by counting the RFUs of DAPI, and the standardized RFUs were calculated as RFUs of ROS relative to time 0.

Improving freeze–thaw tolerance through pre-treatment

Before cell freezing, a stearoyl-coA desaturase (*SCD*) 1 inhibitor (CAY10566, Cayman Chemical, MI, USA) was added to the culture medium of MSCs (2.5 μ M) and HUVECs (25 μ M) for 3 h. After cell detachment, the cells were counted and frozen at 3.0×10^5 cells/250 μ L in 90% FBS, 5% DMSO, and 5 mM GSH (Teva Takeda Pharma Ltd., Aichi, Japan). Freezing and thawing were performed using the same technique described above.

Statistical analysis

Statistical analysis was performed using Prism 9 (GraphPad Inc., La Jolla, CA, USA) and R software (The R Foundation for Statistical Computing, Vienna, Austria). Each statistical test used is described in the respective figure legend. Statistical significance was set at $p < 0.05$.

Results

Freeze–thaw tolerance of MSCs and HUVECs

The live cell rate of synovial MSCs and HUVECs was examined after freeze–thawing (Fig. 1A). FITC[−]V500[−] cells constituted approximately 75% of the MSCs and 60% of the HUVECs (Fig. 1B). Total DNA, RNA, and cellular protein yields from synovial MSCs and HUVECs were measured using cultured and thawed cells (Fig. 1C–E). In HUVECs, RNA and DNA content significantly decreased after freeze–thawing (Fig. 1C and D). In contrast, protein content in MSCs and HUVECs did not significantly decrease after freeze–thawing (Fig. 1E). Analysis of CFUs seeded immediately after freeze–thawing showed that the colony formation capacity of MSCs was maintained after freeze–thawing, whereas that of HUVECs was significantly reduced (Fig. 1F and G). The colony area was decreased in both cells.

Transcriptome analysis was performed to elucidate the alterations in gene expression profiles caused by freeze–thawing. The top 20 GO terms among 342 genes of MSCs and 542 genes of HUVECs were determined after

(See figure on next page.)

Fig. 1 Freeze–thaw tolerance of MSCs and HUVECs. **a** Flow cytometric analysis of synovial MSCs and HUVECs after freeze–thawing. FITC-caspase-3/7 and V500-SYTOX™ blue dead cell staining is shown. **b** Live cell rate of synovial MSCs and HUVECs. Cells negative for FITC and V500 were considered live cells. Mean values and SD are shown ($n = 6$). The p value was calculated using the Mann–Whitney test. **c** RNA content in synovial MSCs and HUVECs (3.0×10^5) before and after freeze–thawing. The mean values and SD are shown ($n = 6$). The p value was calculated using the Mann–Whitney test. **d** DNA content in synovial MSCs and HUVECs (3.0×10^5) before and after freeze–thawing. The mean values and SD are shown ($n = 6$). The p value was calculated using the Mann–Whitney test. **e** Protein concentrations in synovial MSCs and HUVECs (3.0×10^5) before and after freeze–thawing. The mean values and SD are shown ($n = 6$). The p value was calculated using the Mann–Whitney test. **f** Colony forming units (CFUs) of synovial MSCs and HUVECs before and after freeze–thawing. Representative dishes stained with crystal violet are shown. **g** CFUs after 12 days in culture before and after freeze–thawing. The mean values and SD are shown ($n = 18$). **h** Colony area after 12 days in culture before and after freeze–thawing. Mean values and SD are shown ($n = 12$). Cultured: fresh cells as seen before freeze–thawing. Thawed: cells immediately observed after freeze–thawing. The p value was calculated using the Kruskal–Wallis test with the Steel–Dwass multiple comparisons test

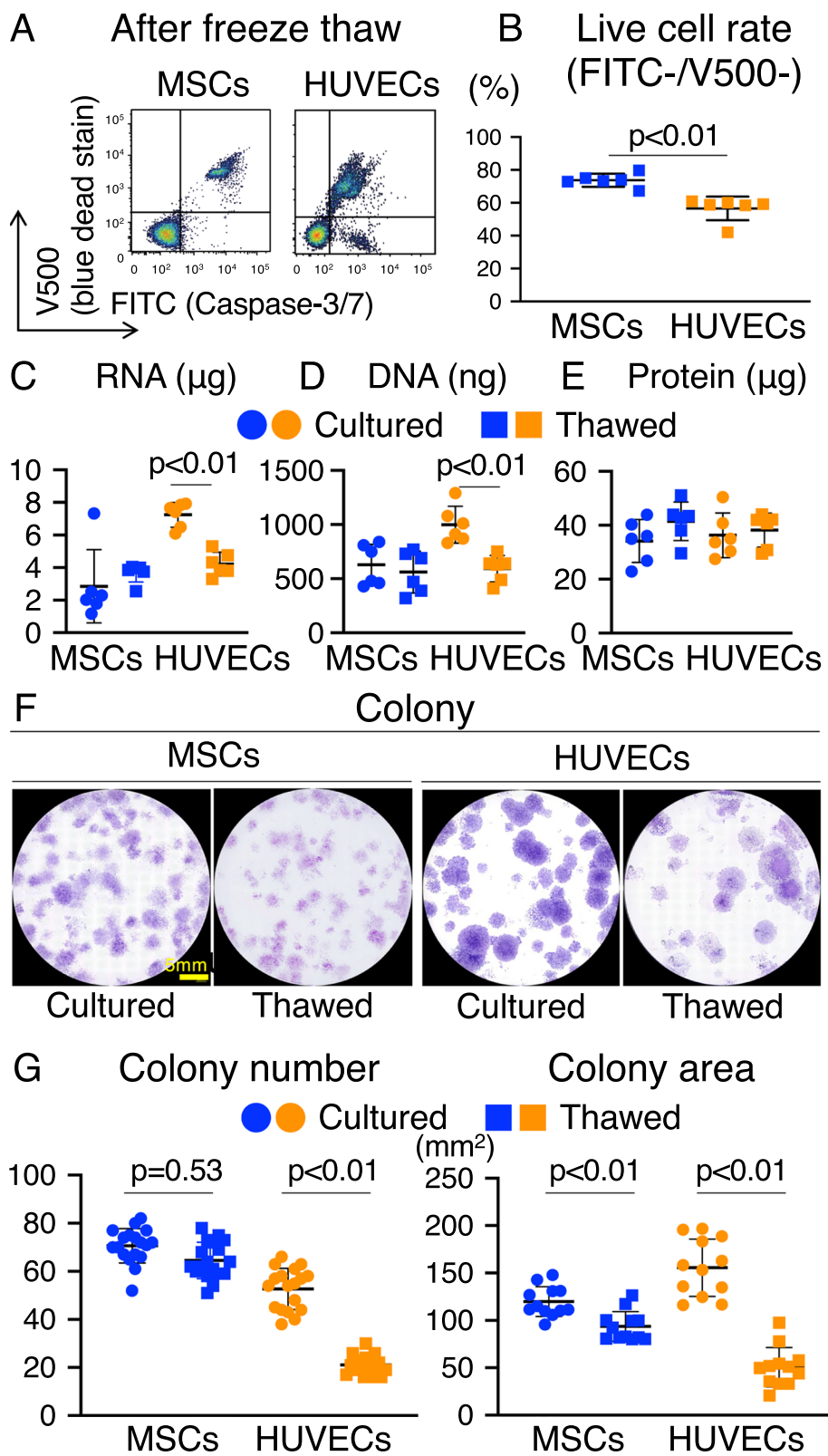


Fig. 1 (See legend on previous page.)

freeze-thawing (Additional file 1: Fig. S1A). We found that 97 genes were commonly altered in the two cell types (Additional file 1: Fig. S1B). These 97 genes indicated that the alterations common to MSCs and HUVECs after freeze-thawing were mostly related to the extracellular matrix (Additional file 1: Fig. S1C).

Alterations in gene expression profiles by DMSO supplementation

To evaluate the effect of DMSO use in the cryopreservation solution, alterations in gene expression were evaluated before and after DMSO supplementation. Venn diagram-based analysis of the transcriptome data revealed a higher number of genes upregulated in HUVECs between 0.5 and 3 h after supplementation with 5% DMSO (562 genes) compared to the overlap with MSCs (17 genes) (Fig. 2A). The expression of AQP1 and AQP5, also called water channels, was increased rapidly in HUVECs after adding 5% DMSO (Additional file 1: Fig. S2). The top 20 GO terms indicated enrichment of the extracellular vesicles and extracellular regions (Fig. 2B). A heatmap from the gene list of extracellular vesicles with the highest enrichment scores showed the fold change of gene expression before and 3 h after DMSO addition. Overall, significant alterations were observed in HUVECs compared to those in MSCs (Fig. 2C).

Cell membrane fluidity before and after DMSO supplementation

Based on the high expression of genes related to extracellular vesicle production, DMSO is considered to interact with the cell membrane as the first interface to tune its physical properties. To elucidate the physical action of DMSO, laurdan microscopy was applied to MSCs and HUVECs to measure membrane fluidity. First, HUVECs were found to have higher fluidity than MSCs (blue cells in Fig. 3A). Although the frequency and position of the first peak in the GP histogram ($GP > 0.3$) were comparable between MSCs and HUVECs (Additional file 1: Fig. S3), the frequency at the second peak of HUVECs in the

high fluidity region ($-6 < GP < 0$) was two times higher than that of MSCs (Fig. 3B). Further, the frequency of HUVECs in the high fluidity region was easily enhanced by adding 5% DMSO, whereas that of MSCs remained intact. Interestingly, high gene expression of stearoyl-CoA desaturase (*SCD1*), an enzyme that produces desaturated fatty acids, was observed in HUVECs compared to MSCs. Addition of a specific *SCD1* inhibitor (CAY10566) suppressed the appearance of cell membranes with high fluidity, even in the presence of DMSO (Fig. 3C). Statistical analysis of histograms clearly indicated that the inhibitor closed the gap in membrane fluidity signature between HUVECs and MSCs and increased tolerance to DMSO (Fig. 3D).

Antioxidant capacity of MSCs and HUVECs

The expression profile of antioxidant-related genes showed that MSCs and HUVECs were characterized differently in the cluster analysis (Fig. 4A). Biochemical analysis revealed that GSH levels and SOD activities of MSCs were significantly higher than those of HUVECs (Fig. 4B), whereas the SOD activity of HUVECs was below the detection limit (Fig. 4C).

The effect of DMSO use in the cryopreservation solution on ROS production was also assessed. ROS production was observed in MSCs and HUVECs before adding 5% DMSO at time 0 and after 3 h. Compared to MSCs, HUVECs treated with 5% DMSO showed more ROS production after 3 h (Fig. 4D). Furthermore, variations in ROS production were not statistically significant in MSCs, whereas ROS production was significantly increased in HUVECs after 1.5 and 3 h (Fig. 4E). GSH levels in MSCs and HUVECs were observed after supplementation with 5% DMSO both at 0 and 0.5 h; however, cells with low fluorescence intensity were present only in HUVECs (Fig. 4F). GSH levels changed over time with the addition of 5% DMSO, but not significantly, in MSCs. On the contrary, GSH levels significantly decreased after 0.5 h and remained low after 1.5 h and 3 h in HUVECs (Fig. 4G).

(See figure on next page.)

Fig. 2 Alterations in gene expression profiles by DMSO supplementation. **a** Venn diagram of genes with twofold upregulation after DMSO supplementation. Time 0; before supplementation. **b** GO analyses for differentially expressed genes between before and after DMSO supplementation. The top 20 GO terms with high enrichment scores and low *p* values between the cells before and after DMSO supplementation are shown. **c** Heatmap for the GO1903561 (extracellular vesicle) gene profile of relative fold changes from time 0 to 3 h after DMSO supplementation

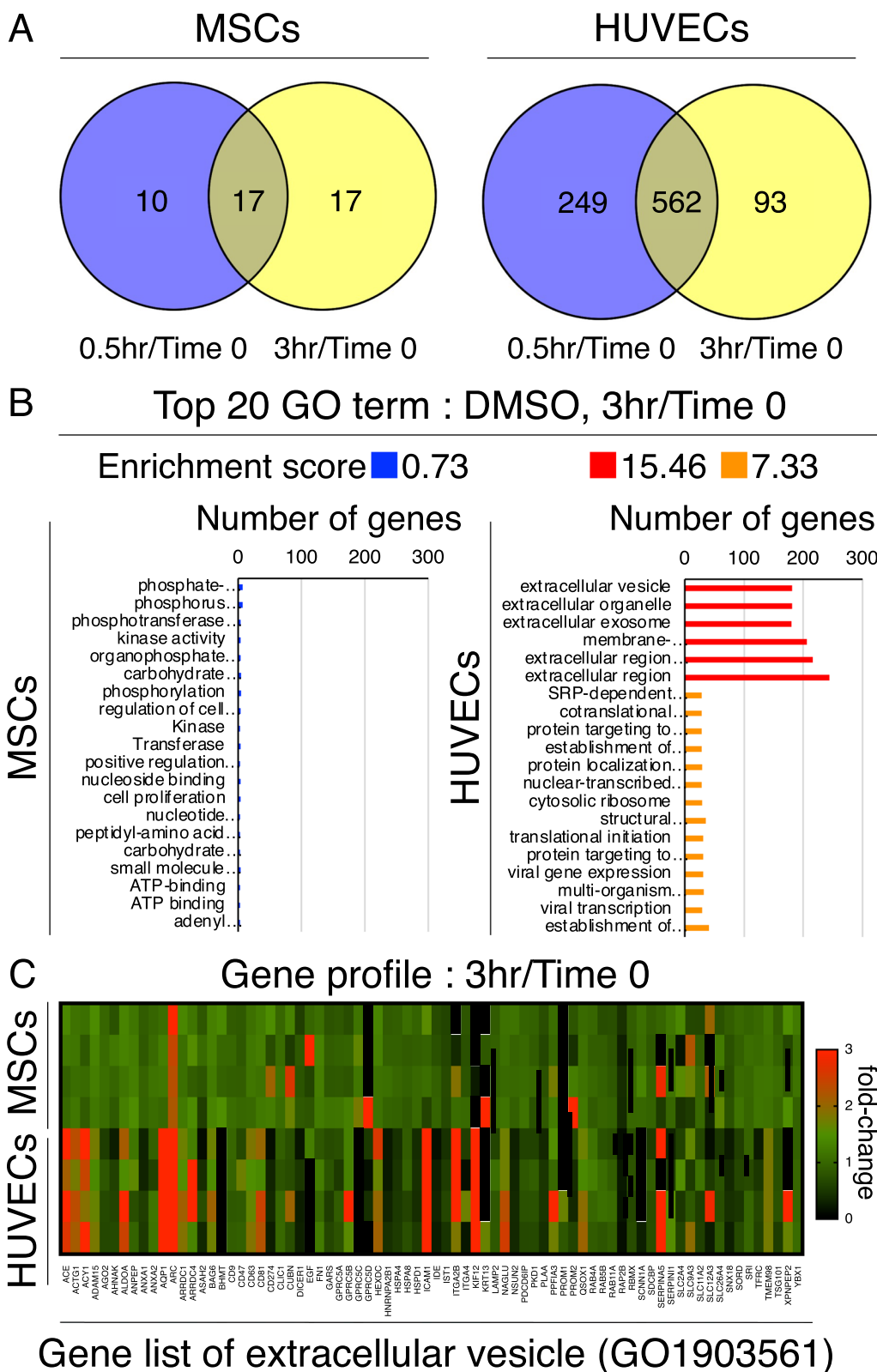


Fig. 2 (See legend on previous page.)

Improving freeze–thaw tolerance through pre-treatment

After controlling cell membrane fluidity using CAY10566 and reducing the damage from ROS using GSH, MSCs and HUVECs were evaluated for live cell rate after freeze–thawing. The combination of CAY10566 and antioxidant GSH treatment significantly improved the ratio of FITC⁻V500⁻ cells immediately after freeze–thawing from $74 \pm 4\%$ to $84 \pm 1\%$ and $57 \pm 7\%$ to $69 \pm 4\%$ in MSCs and HUVECs, respectively (Fig. 5A and B). Analysis of CFUs seeded immediately after freeze–thaw treatment showed that the colony formation capacity of HUVECs was increased after treatment with CAY10566 and GSH (Fig. 5C and D). The colony area was also significantly increased in HUVECs (Fig. 5C and D). These results clearly indicate that controlling the physical and biological properties of cells can improve freeze–thaw tolerance.

Discussion

We found that differences in resistance to DMSO between MSCs and HUVECs is a biological and physical factor controlling freezing tolerance. DMSO protects cells by making the preservation solution highly osmotic, thereby removing water from cells and preventing the formation of ice crystals [10–12]. However, some cell types are severely impaired by DMSO function. HUVECs showed lower freeze–thaw tolerance than MSCs, and the variation in gene expression was significantly affected by DMSO addition. Analysis of cell membrane fluidity showed a larger number of cells with high fluidity among HUVECs than among MSCs, and fluidity was easily enhanced by the addition of DMSO. HUVECs were also less tolerant to ROS generation, which is known to be one of the common toxicity mechanisms of DMSO. Considering the low activities of GSH and SOD in HUVECs, which reduce ROS, DMSO can easily cause cytotoxicity. The freeze–thaw tolerance of HUVECs was improved by (1) controlling their cell membrane fluidity, thus reducing the effect of DMSO, and (2) suppressing the internal ROS-driven cytotoxicity using GSH.

Unlike MSCs, HUVECs showed significantly decreased live cell rate, colony forming ability, and colony area after freeze–thawing. Thus, HUVECs were more negatively affected by freeze–thawing than MSCs. Cell viability is generally reduced by freeze–thawing in any cell type. Water influx into cells is one of the main factors for cryoinjury. Cryoprotectants accelerate water loss; however, excessive water loss causes shrinkage of cells below a lethal minimum volume [30]. The water permeability of cells is dependent on the cell type [31, 32]. The water permeability of MSCs and HUVECs is affected by their original in vivo environment. Conventionally, synovial MSCs exist in the knee joint with abundant joint fluid, which is a highly osmotic environment in the body due to the presence of an extracellular matrix (e.g., hyaluronic acid). Therefore, the cell membrane of MSCs may originally have high osmotic tolerance and low water permeability. The osmolality of blood, where HUVECs are found, is 280 mOsm/kg H₂O, whereas that of the joint fluid harboring synovial MSCs is 400 mOsm/kg H₂O [33, 34]. In vivo, synovial MSCs are always exposed to high osmotic pressure from joint fluid and may originally be tolerant to the hyperosmotic environment formed by DMSO, which has an osmolality of 700–1000 mOsm/kg H₂O. Therefore, MSCs may inhibit excessive water influx and minimize injury after freeze–thawing.

Although DMSO is the most common cryoprotectant, its toxicity has been indicated in various studies [13, 14]. In the present study, the alteration of gene expression at 30 min and 3 h after addition of 5% DMSO was analyzed in MSCs and HUVECs. The expression of a large number of genes was altered in HUVECs, whereas fewer gene changes were observed in MSCs. Furthermore, the expression of the water channels, AQP1 and AQP5, was increased in HUVECs, suggesting that a large amount of water loss and/or influx occurred in HUVECs [35]. GO term analysis showed that the fluctuating genes were mainly related to the extracellular region, indicating that a large amount of intracellular water loss and excessive

(See figure on next page.)

Fig. 3 Cell membrane fluidity before and after DMSO supplementation. **a** Representative generalized polarization (GP) images of MSCs and HUVECs in the absence/presence of DMSO. **b** Histogram for GP frequency with mean values and SD ($n = 3$). The p value was calculated using the Kolmogorov–Smirnov test. **c** Representative GP images of MSCs and HUVECs in the absence/presence of DMSO and CAY10566 (stearoyl-coA desaturase 1 inhibitors). **d** Histogram for GP frequency showing the mean values and SD ($n = 3$). The p value was calculated using the Kolmogorov–Smirnov test

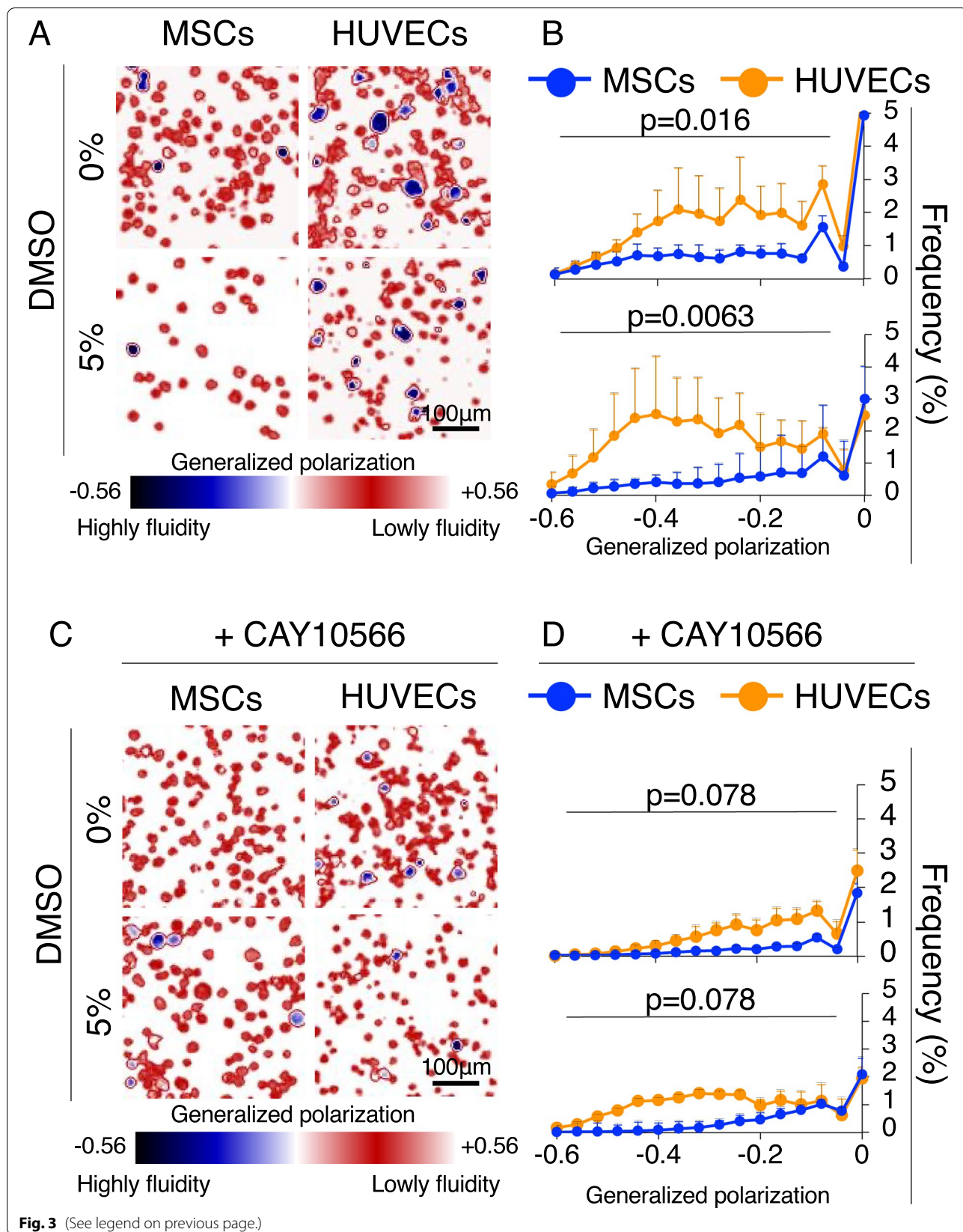


Fig. 3 (See legend on previous page.)

cell shrinkage induced significant extracellular-related gene changes upon DMSO addition.

GO term analysis indicated that extracellular vesicle-related genes constituted the most altered gene set in HUVECs upon DMSO addition. Extracellular vesicles are bilayered lipid membrane particles that carry specific proteins or RNAs and are released upon various external stimuli. The release of extracellular vesicles by murine BV-2 microglial cells and astrocytes is increased by ethanol treatment, and the content of the vesicles is enriched in inflammatory-related proteins and miRNAs related to immune response activation [36, 37]. Therefore, extracellular vesicles are also expected to play a role as biomarkers of disease states [38]. In this study, small vesicle-like structures were observed around HUVECs after DMSO addition. Similar to the response of rat hepatocytes to ethanol treatment [39], the HUVEC membrane fluidity and ROS generation were altered upon DMSO addition. Hence, the increased expression of extracellular vesicle-related genes may be a secondary response caused by excessive water loss by the cell and shrinkage.

DMSO interacts with the cell membrane as the first interface. Indeed, DMSO is known to have a significant effect on the cell membrane, for example, by creating pores in the phospholipid bilayers and altering the water permeability of the cell membrane [40–43]. However, the correlation between cell membrane fluidity and DMSO reactivity in MSCs and HUVECs has not been fully elucidated. In the present study, MSCs showed lower cell membrane fluidity than HUVECs. The membrane fluidity of HUVECs was enhanced by adding 5% DMSO, whereas the membrane fluidity of MSCs was not significantly affected. An increase in membrane fluidity has been considered to cause pore formation in the membrane, facilitating the influx of extracellular solutes [44, 45]. This excessive extracellular solute entry may have caused larger gene expression changes in HUVECs

responding to DMSO, as their fluidity is different from that of MSCs. Cell membrane fluidity is significantly influenced by the expression level of stearoyl-coA desaturase (*SCD1*) [18, 46, 47] (Additional file 1: Fig. S4). Regulation of membrane fluidity in HUVECs via inhibition of *SCD1* by CAY10566 resulted in the membrane fluidity of HUVECs being comparable to that of MSCs. After CAY10566 treatment, the membrane fluidity of HUVECs in response to DMSO was significantly suppressed. These results clearly suggest that HUVEC membrane fluidity is regulated by *SCD1*, and that inhibition of *SCD1* leads to DMSO tolerance.

Differences in cell membrane fluidity between different cell types are closely related to their characteristics. For example, a comparison between undifferentiated and differentiated cells, from induced pluripotent stem cells to endodermal cells, revealed that differentiated cells have lower membrane fluidity [18]. In this study, we focused on the relationship between the original characteristics of each cell type and freeze–thaw tolerance. Differentiation changes the properties of cells, possibly affecting their freeze–thaw tolerance. Therefore, evaluating the original properties and freeze–thaw tolerance of each cell type will provide important information for the design of a manufacturing protocol for therapeutic cells.

ROS generation, a toxic effect of DMSO, is highly damaging to cells [48, 49]. In the current study, the amount of ROS generated by MSCs and HUVECs differed due to differences in antioxidant capacity; MSCs possessed high antioxidant capacity, as reported in previous studies [50–52]. HUVECs had low antioxidant capacity and were possibly damaged by ROS. Decreasing the DMSO concentration could reduce the amount of ROS generated; however, it would not be sufficient to maintain the osmotic pressure required for freezing, resulting in greater damage from intracellular ice formation. Several researchers have attempted to improve the viability of

(See figure on next page.)

Fig. 4 Antioxidant capacity of MSCs and HUVECs after DMSO supplementation. **a** Heatmap for expression profile of antioxidant-related genes. Cluster analyses are based on the expression profiles. FPKM: Fragments Per Kilobase of exon per Million mapped reads. **b** Amount of GSH in MSC and HUVEC lysates. Mean values and SD are shown ($n = 4$). The p value was calculated using the Mann–Whitney test. **c** Superoxide dismutase (SOD) activity in MSC and HUVEC lysates. Mean values and SD are shown ($n = 6$). The p value was calculated using the Mann–Whitney test. **d** Representative images of ROS (green) and cell nuclei stained with DAPI (blue). Data at time 0 and 3 h after supplementation with 5% DMSO are shown. **e** Alteration in ROS levels by 5% DMSO supplementation. Data are shown as relative fluorescence unit (RFU) values. $*p < 0.05$. The p value was calculated by two-way ANOVA with Dunnett's multiple comparisons test. **f** Representative images of glutathione (GSH) (blue). Data at time 0 and 0.5 h after supplementation with 5% DMSO are shown. **g** Alterations in GSH levels by 5% DMSO supplementation. Data are shown as RFU values. $*p < 0.05$. The p value was calculated by two-way ANOVA with Dunnett's multiple comparisons test

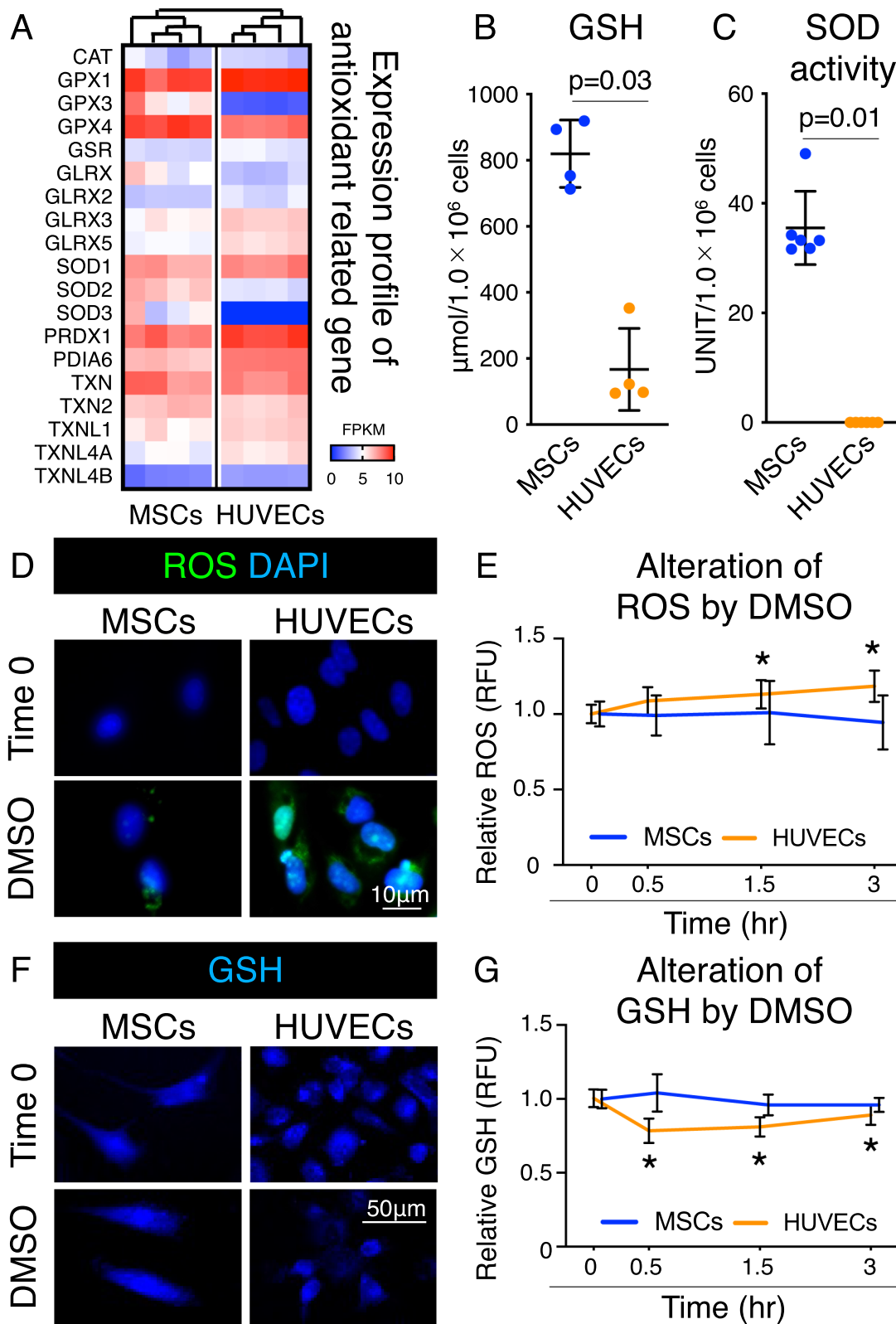


Fig. 4 (See legend on previous page.)

cells by adding antioxidants (e.g., GSH and catalase) to the cryopreservation solution for suppressing ROS generation [53–55]. Further, strict temperature control using programmed freezers also attenuates intracellular ice formation [5]. To clarify resistance to DMSO, it is important to preliminarily evaluate the antioxidant properties of target cells before cryopreservation, considering both the physical and biological aspects.

Pre-treatment with CAY10566 (*SCD1* inhibitor) and addition of GSH (antioxidant) to the cryopreservation solution was found to significantly improve freeze–thaw tolerance. These treatments improved the survival rates of MSCs and HUVECs after freeze–thawing. In particular, colony forming ability and colony area of HUVECs were significantly improved, whereas MSCs showed a tendency to improve, but not significantly. GSH, one of the most abundant low-molecular-weight antioxidants, has the ability to remove ROS [56], which may also have improved the viability of HUVECs in the current study. CAY10566 is an inhibitor of *SCD1*, which catalyzes the biosynthesis of saturated fatty acids to monounsaturated fatty acids. The fluidity of cell membranes possibly reflects the amount of saturated to monounsaturated fatty acids; thus, the expression level of *SCD1* contributes to cell membrane fluidity [57]. In the current study, altering the components of the phospholipid bilayer of HUVECs resulted in a fluidity comparable to that of MSCs. Our results suggest that these changes suppressed the action of DMSO and improved cell survival.

This study had three limitations. First, the improvement in cell viability was limited and was not recovered to the cell viability level before freezing. It is thus possible that other factors may have influenced freeze–thaw tolerance. Cell surface biophysical properties are a candidate for influencing resistance to the ice crystals produced during freezing. For example, a factor directly related to ice crystal formation is proposed as the physical distance of the gap junction between cell membranes [58]. To understand the freeze–thaw tolerance of cells, it is necessary to analyze the molecular mechanisms as well as the biophysics of cells. Second,

no cytoskeleton analysis was performed in this study. The cytoskeleton is known to be disrupted after freeze–thawing [59]. Alterations in the cytoskeleton such as blebbing have also been observed due to freeze–thawing and osmotic responses [60, 61]. Using a Rock inhibitor (Y27632), acting disruption has been shown to decrease, and this treatment improves survival rate after freeze–thawing [62]. Therefore, additional combination of a Rock inhibitor targeting the cytoskeletal effects in HUVECs may effectively improve the cell survival rate. Third, in addition to CAY10566, several other reagents can control cell membrane fluidity. For example, epigallocatechin gallate (EGCG) is an antioxidant [63, 64] that can decrease cell membrane fluidity [65, 66]. In human osteosarcoma cells, EGCG was found to suppress the growth inhibition that occurs during repeated freeze–thaw cycles [67]. Therefore, freeze–thaw tolerance may be improved by evaluating various reagents that control cell membrane fluidity.

Conclusion

We found that MSCs and HUVECs differed in their resistance to DMSO when used as a cryoprotectant, and that their DMSO tolerance depended on cell membrane fluidity and ROS resistance (Fig. 6). The findings suggest that DMSO acts on the lipid-rich cell membrane of HUVECs, increasing the fluidity of the cell membrane. This higher fluidity leads to the formation of a pore-induced DMSO influx into the cytoplasm, which enhances ROS production and induces greater cytotoxicity in HUVECs, which have lower antioxidant capacity than MSCs. In conclusion, cell-specific differences in freeze–thaw tolerance originate from differences in cell membrane fluidity and antioxidant capacity. By demonstrating the efficacy of analyzing the freeze–thaw tolerance of cells from the viewpoint of both biology and membrane-physics, our findings provide a basis for establishing appropriate cryopreservation procedures and promoting cell transplantation therapies.

(See figure on next page.)

Fig. 5 Improving freeze–thaw tolerance through pre-treatment. **a** Flow cytometric analysis of synovial MSCs and HUVECs after freeze–thawing by forward scatter (FSC) and side scatter (SSC), stained with FITC-caspase-3/7 and V500-SYTOX™ blue dead cell stain. **b** Live cell rate of synovial MSCs and HUVECs. Cells negative for FITC and V500 were considered live cells. Mean values and SD are shown ($n=6$). The p value was calculated using the Mann–Whitney test. **c** Colony forming units (CFUs) of synovial MSCs and HUVECs after freeze–thawing. Representative dishes stained with crystal violet. **d** CFUs after 12 days in culture before and after freeze–thawing. Mean values and SD are shown ($n=18$). **e** Colony area after 12 days in culture before and after freeze–thawing. Mean values and SD are shown ($n=12$). Thawed: cells immediately after freeze–thawing. The p value was calculated using the Kruskal–Wallis test with Steel–Dwass multiple comparisons test

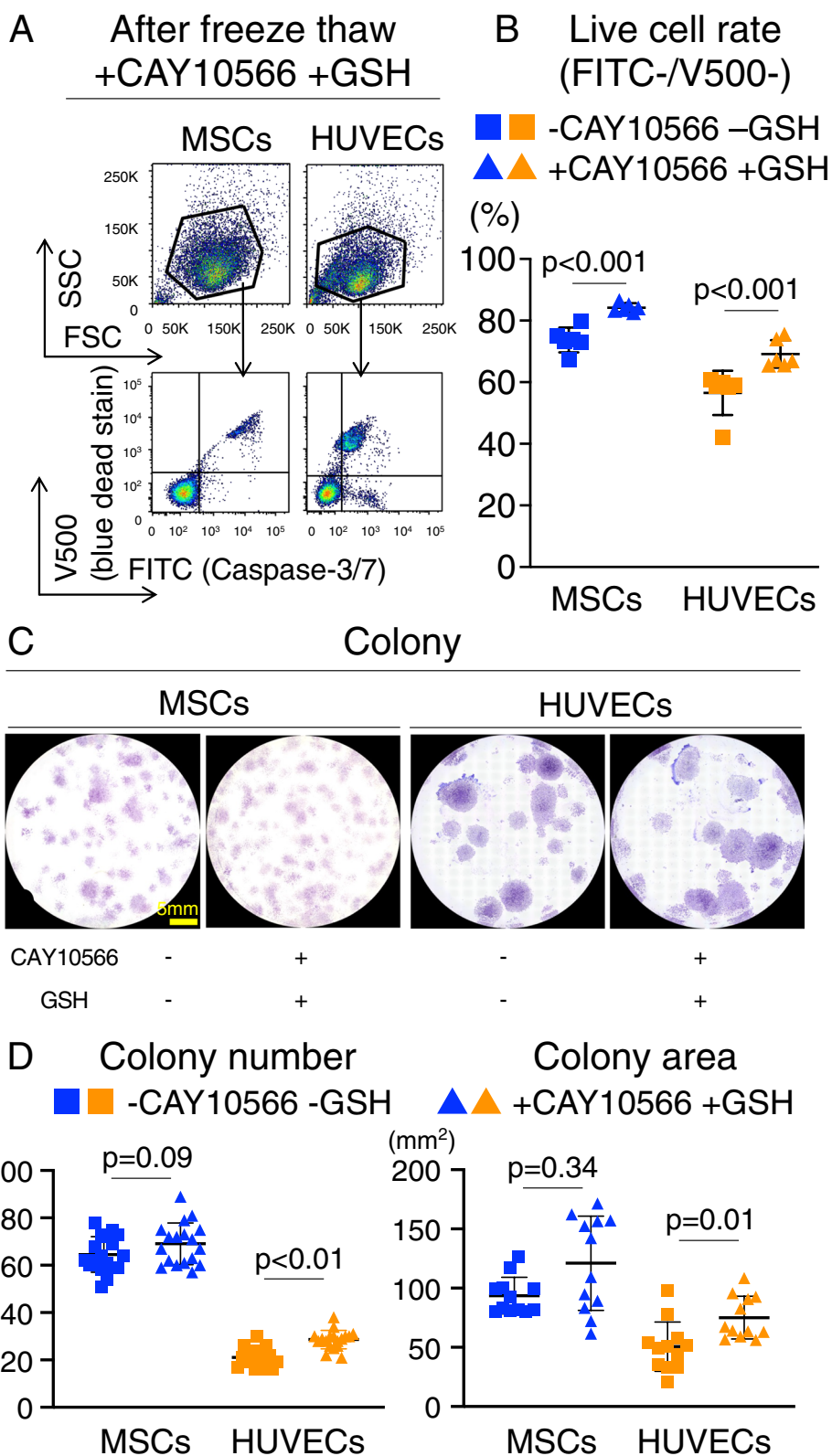
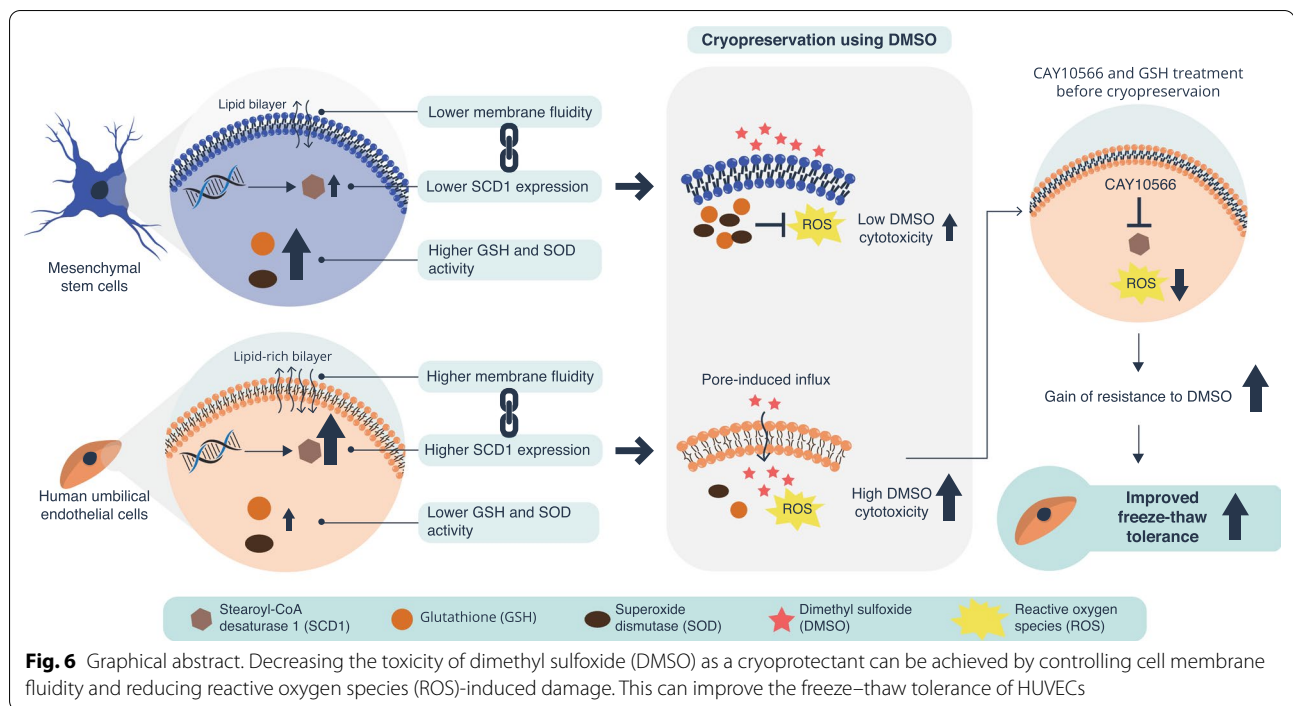


Fig. 5 (See legend on previous page.)



Abbreviations

MSC: Mesenchymal stem cell; HUVEC: Human umbilical vein endothelial cell; DMSO: Dimethyl sulfoxide; SCD1: Stearoyl-coA desaturase; GSH: Glutathione; ROS: Reactive oxygen species; RFU: Relative fluorescence unit; CFU: Colony forming unit; GP: Generalized polarization; SOD: Superoxide dismutase; GO: Gene ontology; AQP: Aquaporin; EGCG: Epigallocatechin gallate.

Supplementary Information

The online version contains supplementary material available at <https://doi.org/10.1186/s13287-022-02850-y>.

Additional file 1: Figure S1. Alteration of mRNA expression profiles after freeze-thawing. (a) GO analyses for differentially expressed genes between cells before and after freeze-thawing. The top 15 GO terms with high enrichment scores and low *p* values between freeze-thawed and fresh cells are shown. (b) Venn diagram of genes with twofold upregulation after freeze-thawing in MSCs and HUVECs. (c) GO terms with high enrichment scores and low *p* values for the 97 co-expressed genes in MSCs and HUVECs. **Figure S2.** Differences in AQP expression after supplementation with 5% DMSO between MSCs and HUVECs. **Figure S3.** Cell membrane fluidity. (a) Low magnification histograms for frequency by GP are shown with mean \pm SD ($n = 3$). Data are shown for conditions before and after DMSO supplementation. (b) Low magnification histograms for frequency by GP are shown with mean \pm SD ($n = 3$). Data are shown in the absence/presence of DMSO and CAY10566 (stearoyl-coA desaturase 1 inhibitors). **Figure S4.** Differences in lipogenesis between MSCs and HUVECs.

Acknowledgements

We thank Kimiko Takanashi for the management of our laboratory. We also thank Seiichiro Nakabayashi for the use of equipment and support of research activities. We would like to thank Wiley Editing Services for English language editing.

Author contributions

MM conceived the study, designed the experiments, collected and analyzed the data, has full access to all the data in the study, and takes responsibility for

the integrity of the data and the accuracy of the data analysis. TM conducted membrane fluidity analysis and wrote the manuscript. NO, HKa, HKo, and IS recruited the patients, acquired the clinical samples, and revised the manuscripts. TT and HYY provided analytical equipment and environment, support for analysis, and revised the manuscripts. MM and IS drafted and wrote the paper. IS provided advice regarding the research strategy, and analytical equipment and environment. All authors were involved in drafting the article or revisited it critically for important intellectual content, and all authors approved the final version to be published.

Funding

This study was supported by JSPS KAKENHI Grant Numbers 16H06262 and 19K18453 to MM, 21H03790 to TM, and the Japan Science and Technology Agency-FOREST Grant Number JPMJFR205N to TM.

Availability of data and materials

The data set supporting the results of RNA-sequence is available in the Open Science Framework repository: <https://doi.org/10.17605/OSF.IO/VF2MR>.

Declarations

Ethics approval and consent to participate

All methods were carried out in accordance with relevant guidelines and regulations. All procedures performed in the study involving human participants were in accordance with the declaration of Helsinki. This study was approved by the Medical Research Ethics Committee of Tokyo Medical and Dental University (M2017-142), and informed consent was obtained from all study subjects.

Consent for publication

Not applicable.

Competing interests

The authors declare that they have no competing interests.

Author details

¹Center for Stem Cell and Regenerative Medicine, Tokyo Medical and Dental University (TMDU), 1-5-45, Bunkyo-ku, Yushima, Tokyo 113-8510, Japan.

²Division of Strategic Research and Development, Graduate School of Science and Engineering, Saitama University, 255, Shimo-okubo, Sakura-ku, Saitama City, Saitama 338-8570, Japan. ³Institute of Research, Tokyo Medical and Dental University (TMDU), Tokyo, Japan. ⁴Department of Applied Physics, Graduate School of Engineering, Osaka University, 2-1, Yamadaoka, Suita City, Osaka 565-0871, Japan. ⁵Department of Joint Surgery and Sports Medicine, Graduate School, Tokyo Medical and Dental University (TMDU), 1-5-45, Bunkyo-ku, Yushima, Tokyo 113-8519, Japan. ⁶Organoid Medicine Project, T-CiRA Joint Program, Fujisawa, Kanagawa, Japan. ⁷Division of Gastroenterology, Hepatology and Nutrition and Division of Developmental Biology, Cincinnati Children's Hospital Medical Center (CCHMC), Cincinnati, OH, USA. ⁸The Center for Stem Cell and Organoid Medicine (CuSTOM), Cincinnati Children's Hospital Medical Center, Cincinnati, OH, USA. ⁹Department of Pediatrics, University of Cincinnati College of Medicine, Cincinnati, OH, USA. ¹⁰Department of Chemistry, Saitama University, 255, Shimo-okubo, Sakura-ku, Saitama City, Saitama 338-8570, Japan.

Received: 3 September 2021 Accepted: 21 March 2022

Published online: 03 May 2022

References

- Jang TH, Park SC, Yang JH, Kim JY, Seok JH, Park US, et al. Cryopreservation and its clinical applications. *Integr Med Res.* 2017;6:12–8.
- Asghar W, El Assal R, Shafiee H, Anchan RM, Demirci U. Preserving human cells for regenerative, reproductive, and transfusion medicine. *Biotechnol J.* 2014;9:895–903.
- Fujisawa R, Mizuno M, Katano H, Otabe K, Ozeki N, Tsuji K, et al. Cryopreservation in 95% serum with 5% DMSO maintains colony formation and chondrogenic abilities in human synovial mesenchymal stem cells. *BMC Musculoskelet Disord.* 2019;20:1–9.
- Horiuchi K, Ozeki N, Endo K, Mizuno M, Katano H, Akiyama M, et al. Thawed cryopreserved synovial mesenchymal stem cells show comparable effects to cultured cells in the inhibition of osteoarthritis progression in rats. *Sci Rep.* 2021;11:1–14.
- Sultani AB, Marquez-Curtis LA, Elliott JAW, McGann LE. Improved cryopreservation of human umbilical vein endothelial cells: a systematic approach. *Sci Rep.* 2016;6:1–14.
- Takebe T, Sekine K, Enomura M, Koike H, Kimura M, Ogaeri T, et al. Vascularized and functional human liver from an iPSC-derived organ bud transplant. *Nature.* 2013;499:481–4.
- Takebe T, Kobayashi S, Suzuki H, Mizuno M, Chang Y-M, Yoshizawa E, et al. Transient vascularization of transplanted human adult-derived progenitors promotes self-organizing cartilage. *J Clin Investig.* 2014;124:4325–34.
- Awan M, Buriak I, Fleck R, Fuller B, Goltsev A, Kerby J, et al. Dimethyl sulfoxide: a central player since the dawn of cryobiology, is efficacy balanced by toxicity? *Regen Med.* 2020;15:1463–91.
- Marquez-Curtis LA, Janowska-Wieczorek A, McGann LE, Elliott JAW. Mesenchymal stromal cells derived from various tissues: biological, clinical and cryopreservation aspects. *Cryobiology.* 2015;71:181–97.
- Muldrew K, McGann LE. Mechanisms of intracellular ice formation. *Biophys J.* 1990;57:525–32.
- Fowler A. Cryo-Injury and biopreservation. *Ann N Y Acad Sci.* 2005;1066:119–35.
- Gao D, Critser JK. Mechanisms of cryoinjury in living cells. *ILAR J.* 2000;41:187–96.
- Galvao J, Davis B, Tilley M, Normando E, Duchon MR, Cordeiro MF. Unexpected low-dose toxicity of the universal solvent DMSO. *FASEB J.* 2013;28:1317–30.
- Best BP. Cryoprotectant toxicity: facts, issues, and questions. *Rejuvenation Res.* 2015;18:422–36.
- Buch SJ, Yuan C, Gao J, Guo J, Bai L, Marshall C, et al. Dimethyl Sulfoxide Damages Mitochondrial Integrity and Membrane Potential in Cultured Astrocytes. *PLoS ONE.* 2014;9:e107447.
- Ock S-A, Rho G-J. Effect of dimethyl sulfoxide (DMSO) on cryopreservation of porcine mesenchymal stem cells (pMSCs). *Cell Transpl.* 2011;20:1231–9.
- Sumida K, Igarashi Y, Toritsuka N, Matsushita T, Abe-Tomizawa K, Aoki M, et al. Effects of DMSO on gene expression in human and rat hepatocytes. *Hum Exp Toxicol.* 2011;30:1701–9.
- Matsuzaki T, Matsumoto S, Kasai T, Yoshizawa E, Okamoto S, Yoshikawa HY, et al. Defining lineage-specific membrane fluidity signatures that regulate adhesion kinetics. *Stem Cell Rep.* 2018;11:852–60.
- Schaeffer BE, Curtis AS. Effects on cell adhesion and membrane fluidity of changes in plasmalemmal lipids in mouse L929 cells. *J Cell Sci.* 1977;26:47–55.
- Edmond V, Dufour F, Poiroux G, Shoji K, Malleter M, Fouqué A, et al. Downregulation of ceramide synthase-6 during epithelial-to-mesenchymal transition reduces plasma membrane fluidity and cancer cell motility. *Oncogene.* 2014;34:996–1005.
- Silberman S, McGarvey TW, Comrie E, Persky B. The influence of ethanol on cell membrane fluidity, migration, and invasion of murine melanoma cells. *Exp Cell Res.* 1990;189:64–8.
- Giraud MN. Membrane fluidity predicts the outcome of cryopreservation of human spermatozoa. *Hum Reprod.* 2000;15:2160–4.
- Peris-Frau P, Soler AJ, Iniesta-Cuerda M, Martín-Maestro A, Sánchez-Ajofrín I, Medina-Chávez DA, et al. Sperm cryodamage in ruminants: understanding the molecular changes induced by the cryopreservation process to optimize sperm quality. *Int J Mol Sci.* 2020;21:2781.
- Mizuno M, Katano H, Shimozaki Y, Sanami S, Ozeki N, Koga H, et al. Time-lapse image analysis for whole colony growth curves and daily distribution of the cell number per colony during the expansion of mesenchymal stem cells. *Sci Rep.* 2019;9:1–9.
- Mizuno M, Endo K, Katano H, Amano N, Nomura M, Hasegawa Y, et al. Transplantation of human autologous synovial mesenchymal stem cells with trisomy 7 into the knee joint and 5 years of follow-up. *Stem Cells Transl Med.* 2021;10:1530–43.
- Huang DW, Sherman BT, Lempicki RA. Systematic and integrative analysis of large gene lists using DAVID bioinformatics resources. *Nat Protoc.* 2008;4:44–57.
- Parasassi T, De Stasio G, Ravagnan G, Rusch RM, Gratton E. Quantitation of lipid phases in phospholipid vesicles by the generalized polarization of Laurdan fluorescence. *Biophys J.* 1991;60:179–89.
- Gaus K, Gratton E, Kable EPW, Jones AS, Gelissen I, Kritharides L, et al. Visualizing lipid structure and raft domains in living cells with two-photon microscopy. *Proc Natl Acad Sci.* 2003;100:15554–9.
- Owen DM, Rentero C, Magenau A, Abu-Siniyeh A, Gaus K. Quantitative imaging of membrane lipid order in cells and organisms. *Nat Protoc.* 2011;7:24–35.
- Mazur P. Freezing of living cells: mechanisms and implications. *Am J Physiol Cell Physiol.* 1984;247:C125–42.
- Moshelion M, Moran N, Chaumont F. Dynamic changes in the osmotic water permeability of protoplast plasma membrane. *Plant Physiol.* 2004;135:2301–17.
- Boss D, Kühn J, Jourdain P, Depeursinge C, Magistretti PJ, Marquet P. Measurement of absolute cell volume, osmotic membrane water permeability, and refractive index of transmembrane water and solute flux by digital holographic microscopy. *J Biomed Opt.* 2013;18:036007.
- Shanfield S, Campbell P, Baumgarten M, Bloebaum R, Sarmiento A. Synovial fluid osmolality in osteoarthritis and rheumatoid arthritis. *Clin Orthop Relat Res.* 1988;235:289–95.
- Baumgarten M, Bloebaum RD, Ross SD, Campbell P, Sarmiento A. Normal human synovial fluid: osmolality and exercise-induced changes. *J Bone Joint Surg.* 1985;67:1336–9.
- Takata K. Aquaporins: water channel proteins of the cell membrane. *Prog Histochem Cytochem.* 2004;39:1–83.
- Ibáñez F, Montesinos J, Area-Gomez E, Guerri C, Pascual M. Ethanol induces extracellular vesicle secretion by altering lipid metabolism through the mitochondria-associated ER membranes and sphingomyelinases. *Int J Mol Sci.* 2021;22:8438.
- Ibáñez F, Montesinos J, Ureña-Peralta JR, Guerri C, Pascual M. TLR4 participates in the transmission of ethanol-induced neuroinflammation via astrocyte-derived extracellular vesicles. *J Neuroinflamm.* 2019;16:1–14.

38. Thompson AG, Gray E, Heman-Ackah SM, Mäger I, Talbot K, Andaloussi SE, et al. Extracellular vesicles in neurodegenerative disease—pathogenesis to biomarkers. *Nat Rev Neurol*. 2016;12:346–57.
39. Sergent O, Pereira M, Belhomme C, Chevanne M, Huc L, Lagadic-Gossmann D. Role for membrane fluidity in ethanol-induced oxidative stress of primary rat hepatocytes. *J Pharmacol Exp Ther*. 2005;313:104–11.
40. Colombo G, de Ménorval M-A, Mir LM, Fernández ML, Reigada R. Effects of dimethyl sulfoxide in cholesterol-containing lipid membranes: a comparative study of experiments in silico and with cells. *PLOS ONE*. 2012;7:41733.
41. Raju R, Torrent-Burgués J, Bryant G. Interactions of cryoprotective agents with phospholipid membranes: a Langmuir monolayer study. *Chem Phys Lipids*. 2020;231:e104949.
42. Hughes ZE, Mark AE, Mancera RL. Molecular dynamics simulations of the interactions of DMSO with DPPC and DOPC phospholipid membranes. *J Phys Chem B*. 2012;116:11911–23.
43. Gironi B, Kahveci Z, McGill B, Lechner B-D, Pagliara S, Metz J, et al. Effect of DMSO on the mechanical and structural properties of model and biological membranes. *Biophys J*. 2020;119:274–86.
44. Gurtovenko AA, Anwar J. Modulating the structure and properties of cell membranes: the molecular mechanism of action of dimethyl sulfoxide. *J Phys Chem B*. 2007;111:10453–60.
45. Notman R, Noro M, O'Malley B, Anwar J. Molecular basis for dimethylsulfoxide (DMSO) action on lipid membranes. *J Am Chem Soc*. 2006;128:13982–3.
46. Guillou H, Rodríguez-Cuenca S, Whyte L, Hagen R, Vidal-Puig A, Fuller M. Stearoyl-CoA desaturase 1 is a key determinant of membrane lipid composition in 3T3-L1 adipocytes. *PLOS ONE*. 2016;11:0162047.
47. Jain P, Nattakom M, Holowka D, Wang DH, Thomas Brenna J, Ku AT, et al. Runx1 role in epithelial and cancer cell proliferation implicates lipid metabolism and Scd1 and Soat1 activity. *Stem Cells*. 2018;36:1603–16.
48. Jeong S-G, Cho G-W. Endogenous ROS levels are increased in replicative senescence in human bone marrow mesenchymal stromal cells. *Biochem Biophys Res Commun*. 2015;460:971–6.
49. Toussaint O, Royer V, Salmon M, Remacle J. Stress-induced premature senescence and tissue ageing. *Biochem Pharmacol*. 2002;64:1007–9.
50. Valle-Prieto A, Conget PA. Human mesenchymal stem cells efficiently manage oxidative stress. *Stem Cells Dev*. 2010;19:1885–93.
51. Vono R, Jover Garcia E, Spinetti G, Madeddu P. Oxidative stress in mesenchymal stem cell senescence: regulation by coding and noncoding RNAs. *Antioxid Redox Signal*. 2018;29:864–79.
52. Klein D, Steens J, Wiesemann A, Schulz F, Kaschani F, Röck K, et al. Mesenchymal stem cell therapy protects lungs from radiation-induced endothelial cell loss by restoring superoxide dismutase 1 expression. *Antioxid Redox Signal*. 2017;26:563–82.
53. Limaye LS. Bone marrow cryopreservation: improved recovery due to bioantioxidant additives in the freezing solution. *Stem Cells*. 1997;15:353–8.
54. Sasnoor LM, Kale VP, Limaye LS. Prevention of apoptosis as a possible mechanism behind improved cryoprotection of hematopoietic cells by catalase and trehalose. *Transplantation*. 2005;80:1251–60.
55. Seo JM, Sohn MY, Suh JS, Atala A, Yoo JJ, Shon Y-H. Cryopreservation of amniotic fluid-derived stem cells using natural cryoprotectants and low concentrations of dimethylsulfoxide. *Cryobiology*. 2011;62:167–73.
56. Dannenmann B, Lehle S, Hildebrand Dominic G, Kübler A, Grondona P, Schmid V, et al. High glutathione and glutathione peroxidase-2 levels mediate cell-type-specific DNA damage protection in human induced pluripotent stem cells. *Stem Cell Rep*. 2015;4:886–98.
57. Ntambi JM, Miyazaki M. Recent insights into stearoyl-CoA desaturase-1. *Curr Opin Lipidol*. 2003;14:255–61.
58. Acker JP, Elliott JAW, McGann LE. Interfacial ice propagation: experimental evidence for ice growth through membrane pores. *Biophys J*. 2001;81:1389–97.
59. Chinnadurai R, Garcia Marco A, Sakurai Y, Lam Wilbur A, Kirk Allan D, Galipeau J, et al. Actin cytoskeletal disruption following cryopreservation alters the biodistribution of human mesenchymal stromal cells in vivo. *Stem Cell Rep*. 2014;3:60–72.
60. Guilak F, Erickson GR, Ting-Beall HP. The effects of osmotic stress on the viscoelastic and physical properties of articular chondrocytes. *Biophys J*. 2002;82:720–7.
61. Ragoonanan V, Hubel A, Aksan A. Response of the cell membrane–cytoskeleton complex to osmotic and freeze/thaw stresses. *Cryobiology*. 2010;61:335–44.
62. Ragoonanan V, Less R, Aksan A. Response of the cell membrane–cytoskeleton complex to osmotic and freeze/thaw stresses. Part 2: The link between the state of the membrane–cytoskeleton complex and the cellular damage. *Cryobiology*. 2013;66:96–104.
63. Chen L. Tea catechins protect against lead-induced cytotoxicity, lipid peroxidation, and membrane fluidity in HepG2 cells. *Toxicol Sci*. 2002;69:149–56.
64. Wang D, Wang Y, Xu S, Wang F, Wang B, Han K, et al. Epigallocatechin-3-gallate Protects against hydrogen peroxide-induced inhibition of osteogenic differentiation of human bone marrow-derived mesenchymal stem cells. *Stem Cells Int*. 2016;2016:1–10.
65. Matsuzaki T, Ito H, Chevreva V, Makky A, Kaufmann S, Okano K, et al. Adsorption of galloyl catechin aggregates significantly modulates membrane mechanics in the absence of biochemical cues. *Phys Chem Chem Phys*. 2017;19:19937–47.
66. Tsuchiya H. Effects of green tea catechins on membrane fluidity. *Pharmacology*. 1999;59:34–44.
67. Han D-W, Kim HH, Lee MH, Baek HS, Lee K-Y, Hyon S-H, et al. Protection of osteoblastic cells from freeze/thaw cycle-induced oxidative stress by green tea polyphenol. *Biotech Lett*. 2005;27:655–60.

Publisher's Note

Springer Nature remains neutral with regard to jurisdictional claims in published maps and institutional affiliations.

Ready to submit your research? Choose BMC and benefit from:

- fast, convenient online submission
- thorough peer review by experienced researchers in your field
- rapid publication on acceptance
- support for research data, including large and complex data types
- gold Open Access which fosters wider collaboration and increased citations
- maximum visibility for your research: over 100M website views per year

At BMC, research is always in progress.

Learn more biomedcentral.com/submissions

